BIOCHEMISTRY
including biophysical chemistry & molecular biology

Article

pubs.acs.org/biochemistry

Structural Basis for Differential Insertion Kinetics of dNMPs Opposite a Difluorotoluene Nucleotide Residue

Shuangluo Xia,[†] Soo Hyun Eom,[‡] William H. Konigsberg,*[,†] and Jimin Wang*[,†]

[†]Department of Molecular Biophysics and Biochemistry, Yale University, New Haven, Connecticut 06520-8114, United States

[‡]School of Life Sciences, Steitz Center for Structural Biology, Gwangju Institute of Science and Technology (SCSB-GIST), 261 Cheomdan-gwagiro, Buk-gu, Gwangju 500-712, Republic of Korea.

Supporting Information

ABSTRACT: We have recently challenged the widely held view that 2,4-difluorotoluene (dF) is a nonpolar isosteric analogue of the nucleotide dT, incapable of forming hydrogen bonds (HBs). To gain a further understanding for the kinetic preference that favors dAMP insertion opposite a templating dF, a result that mirrors the base selectivity that favors dAMP insertion opposite dT by RB69 DNA polymerase (RB69pol), we determined presteady-state kinetic parameters for incorporation of four dNMPs opposite dF by RB69pol and solved the structures of corresponding ternary complexes. We observed that both the F2 and F4 substituent of dF in these structures serve as HB acceptors forming HBs either directly with dTTP and dGTP or indirectly with dATP and dCTP via ordered water molecules. We have defined the shape and chemical features of each dF/dNTP pair in the RB69pol active site without the corresponding phosphodiester-linkage constraints of dF/dNs when they are embedded in isolated DNA duplexes. These features can explain the kinetic preferences exhibited by the templating dF when the nucleotide incorporation is catalyzed by wild type RB69pol or its mutants. We further show that the shapes of the dNTP/dF nascent base pair differ markedly from the corresponding dNTP/dT in the pol active site and that these differences have a profound effect on their incorporation efficiencies.

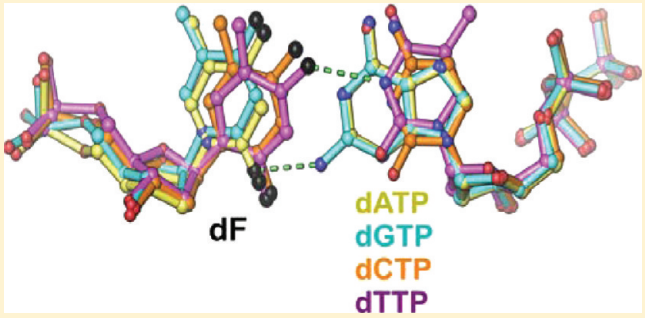

Replicative DNA polymerases, including bacteriophage RB69 DNA polymerase (RB69pol), exhibit an extraordinarily high degree of base selectivity.[1−4] To define the kinetic basis of this selectivity, an array of modified and non-natural nucleobases have been introduced, including 2,4-difluorotoluene nucleoside analogue (dF).[5] Kool and colleagues originally used dF to study the relative importance of shape versus interbase hydrogen bonding (HB) of Watson−Crick (W−C) base pairs (Figure 1A,B), because they reasoned that dF was a "non-polar, non-hydrogen-bonding" isostere of dT.[6−9] The dF analogue differs from dT by four-atom substitutions, F2 and F4 for O2 and O4, C1 and C3 for N1 and N3, respectively. Clearly, the C1 and C3 substitutions for N1 and N3 in the heterocyclic conjugate ring system make it highly hydrophobic by converting it to a toluene derivative. However, the issue of whether the F2 and F4 substituent on the toluene ring of dF have H bonding capability and whether their chemical properties differ from those of the O2 and O4 substituent in dT remain unresolved.[10] The striking similarity of the kinetic preference exhibited by a templating dF and the base selectivity of dT observed with natural dNTPs during primer-extension seemed to support the original hypothesis that dF was a nonpolar isostere of dT.[5,11,12] The kinetic preference shown by dF can be summarized as follows. When this nucleobase analogue is present as a deoxynucleoside triphosphate (dFTP), most pols prefer dFTP over dCTP, dATP, and dGTP for incorporation opposite dA.[11] When dF is present as the templating nucleobase, dATP is preferred over dGTP, dCTP, and dTTP for insertion.[12,13] Furthermore, Kool and colleagues have shown that the shape of the dF/dA pair embedded in an isolated DNA duplex was exactly the same as that of the dT/dA pair, including similar interbase F4/N6 and C3/N1 distances, both of which were within HB distance as in the corresponding O4/N6 and N3/N1 distances of the dT/dA pair but without dF/dA actually forming HBs.[7,14,15] Subsequently, Irimia et al. determined structures of Dpo4 ternary complexes with a template strand that contained dF at the penultimate base pairing position and concluded that Dpo4 used both shape and electrostatics for base discrimination.[16] Dpo4 belongs to a member of the Y family of DNA polymerases and exhibits much reduced base discrimination relative to replicative DNA polymerases such as RB69pol. In addition, Lee et al. investigated the effect of a templating dF on the kinetics exhibited by human mitochondrial pol γ for insertion of natural nucleotides and their analogues.[13,17] Their results suggested that the shape of the nascent base pair was important but

Received: October 31, 2011
Revised: January 27, 2012
Published: January 30, 2012

   dx.doi.org/10.1021/bi2016487 | *Biochemistry* 2012, 51, 1476−1485

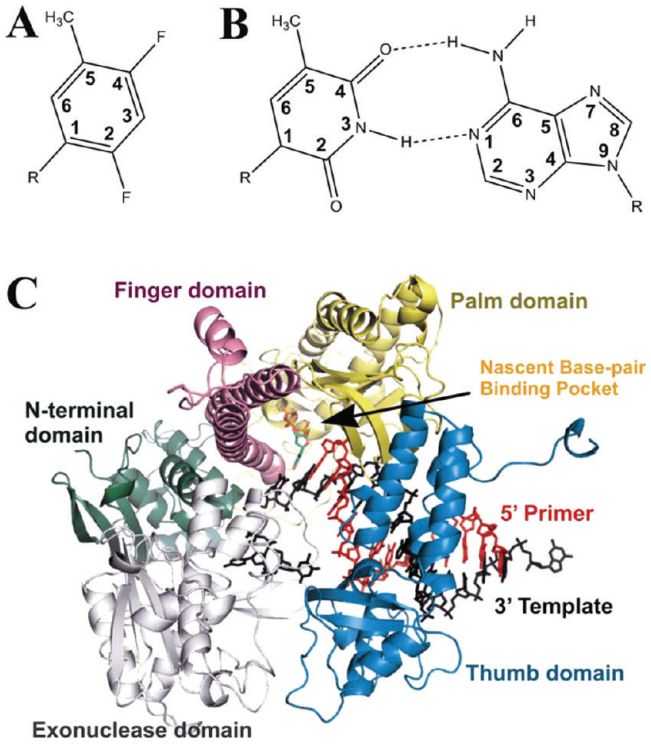

Figure 1. Overall structure of the dF-containing ternary complexes of tm RB69pol. (A) 2,4-Difluorotoluene analogue. (B). Complementary dA/dT base pair. (C). Overview of the dF/dATP complex of tm RB69pol. The pol structure is colored by domains: the N-terminal domain (residues 1−108 and 340−382) in green, Exonuclease (residues 109−339) in gray, Palm (residues 383−468 and 573−729) in yellow, Fingers (residues 469−572) in purple, and Thumb (residues 730−903) in blue. The primer and template strand of the DNA are shown in stick representation with the template in black and the primer in red.

insufficient to explain the efficiency and fidelity of DNA synthesis catalyzed by pol γ. They showed that interbase HBs in the nascent base-pair were responsible for at least a third of the free energy involved in base discrimination and insertion efficiency. Joyce and colleagues have also demonstrated that interbase HBs are important for the polymerase reaction catalyzed by wild type (wt) Klenow fragment, but the requirements of W−C interbase HBs can be relaxed in mutants with enlarged Nascent Base-pair-binding Pockets (NBP).[18]

In this report, we have investigated the kinetic preference of dF by placing it in the templating position of a primer/template (P/T) duplex and asking whether an incoming dNTP in the replicating ternary complex can form HBs with dF (Figure 1C). We selected RB69pol for this study because it is a member of B family DNA polymerases that include human replicative pols.[19] We previously characterized presteady-state kinetic parameters for incorporation of dAMP opposite a templating dF by wt as well as by an RB69pol triple mutant (tm) harboring the L561A/S565G/Y567A substitutions, which increased the NBP volume.[20] Unexpectedly, we found that tm inserted dAMP opposite dF with an efficiency 2,000 fold greater than wt RB69 pol,[20] a finding that runs counter to the concept that incorporation efficiency is coupled to the tightness of fit between a nascent base-pair and the NBP.[21] This phenomenon required a more thorough investigation. Accordingly, we determined presteady-state kinetic parameters for incorporation of all four dNMPs opposite dF by both wt and tm RB69pols. We have also determined the corresponding crystal structures of tm RB69pol ternary complexes containing each of the four-possible dF/dNTP pairs, including the dF/dTTP pair that we have recently reported,[22] in an attempt to correlate the kinetics with structure. Our previously reported dF/dTTP-containing structure demonstrated that dF has H-bonding capability in the environment of a pol active site.[22] The structures reported here provide a basis for understanding why tm and wt RB69pols preferentially incorporate dAMP opposite dF. We also compare the dF/dNTP-containing ternary complexes with the corresponding dT/dNTP-containing ternary complexes and show that the shapes of dF/dNTP pairs are markedly different from dT/dNTP pairs. We suggest that these differences could account for the wide divergence in the kinetic parameters observed for incorporation of dNMPs opposite dF by both tm and wt RB69pols.

EXPERIMENTAL PROCEDURES

Chemicals. All chemicals were the highest quality available; 2′-deoxynucleoside 5′-triphosphates (dNTPs) were purchased from Roche (Roche Applied Science, Indianapolis, IN, USA).

Enzymes. Wt and tm RB69pols as well as the L561A, S565G, and Y567A single mutants and the L561A/Y567A and S565G/Y567A double mutants of RB69pol in the exonuclease-deficient background containing the D222A/D327A substitutions were overexpressed in *E. coli* and purified as previously described.[20,22−25]

P/T DNA Substrates. Oligonucleotides were synthesized by W. M. Keck Foundation Biotechnology Resource Laboratory (Yale University, New Haven, CT, USA). The sequence of one T strand is 5′-TCA(dF)GTAAGCAGTCCGCG-3′, and the sequence of the second T strand differs from the first T template by the replacement of dF with dT; the sequence of one P strand is 5′-GCGGACTGCTTA($_{dd}$C)-3′ with a 3′ dideoxy-terminus for crystallization; the sequence of the second P strand differs from the first P strand with the last ddC being replaced with an extendable dC at the 3′-terminus for kinetic assays. The complementary oligonucleotides were annealed by heating to 95 °C, followed by gradual cooling to 25 °C to give fully duplexed P/Ts.

Crystallization of tm RB69pol Ternary Complexes. For crystallization of ternary complexes, the microbatch vapor-diffusion method was used, and tm RB69pol was mixed in an equal molar ratio with freshly annealed dideoxy-terminated P/T to give a final [RB69pol] of 100 μM. The incoming dNTP (dATP or dCTP) was then added to give a 2 mM final dNTP concentration. The complex containing dGTP was prepared using the soaking-replacement method from the preformed dATP-containing crystals. Equal volumes of a solution containing 150 mM $CaCl_2$, 10% (w/v) poly ethylene glycol 350 monomethyl ether (PEG 350 MME), and 100 mM Na cacodylate (pH 6.5) was added to the RB69pol/P/T/dNTP mixture. Rod-shaped crystals typically grew in 2−3 days at 20 °C. Crystals were then transferred into a cryoprotectant/precipitant solution with the same components but with a higher concentration of PEG350 MME to 30% (w/v) prior to freezing in liquid nitrogen.

X-ray Diffraction Data Collection, Structure Determination, and Refinement. X-ray diffraction data were collected at 110 K at beamline 24ID-E, Northeast Collaborative Access Team (NECAT), Advanced Photon Source, Argonne National Laboratory (APS, ANL, Chicago, IL), and at beamline X-29, National Synchrotron Light Sources (NSLS), Brook-

dx.doi.org/10.1021/bi2016487 | *Biochemistry* 2012, 51, 1476−1485

Table 1. Crystallographic Statistics for Data Collection and Structure Refinement of dF/dNTP-Containing Ternary Complexes Formed by tm RB69pol

	dATP vs dF	dCTP vs dF	dGTP vs dF
space group	$P2_12_12_1$	$P2_12_12_1$	$P2_12_12_1$
unit cell (Å)			
a	78.27	78.35	72.82
b	118.71	118.23	119.98
c	130.52	130.85	130.07
resolution (Å)[a]	50.0−1.96(1.99−1.96)	50.0−2.18(2.27−2.18)	50.0−1.98(2.01−1.98)
no. of unique reflections	82,929	60,226	77,513
redundancy	4.9 (4.5)	5.1 (5.1)	4.8 (4.2)
completeness (%)	99.9 (100.0)	99.7 (99.4)	99.8 (100.0)
R_{merge} (%)[b]	8.9 (95.9)	11.5 (91.9)	12.2 (90.3)
I/σ_I	15.4 (1.2)	14.3 (1.9)	12.1 (1.2)
final model content counts			
amino acid residues	903	903	903
water molecules	911	484	804
Ca^{2+} ions	4	4	5
template nucleotides	18	18	18
primer nucleotides	13	13	13
dNTP molecules	1	1	1
R (%)[c]	17.7 (25.3)	19.0 (24.3)	17.7 (23.8)
R_{free} (%)[c]	21.6 (29.2)	23.8 (28.6)	21.8 (26.5)
R_{o2p}[d]	2.30	1.76	2.16
rmsd[e] for bonds (Å)	0.008	0.008	0.008
rmsd[e] for bond angles (°)	1.108	1.103	1.092
PDB entry	3QER	3QEI	3QES

[a]Statistics for the highest resolution shell are in parentheses. [b]$R_{merge} = \Sigma_{hkl}\Sigma_j |I_j(hkl) - \langle I_j(hkl)\rangle| / \Sigma_{hkl}\Sigma_j \langle I(hkl)\rangle$, statistics for merging all observations for given reflections. [c]$R = \Sigma_{hkl} |F_{obs}(hkl) - F_{calc}(hkl)| / \Sigma_{hkl} F_{obs}(hkl)$, statistics for crystallographic agreement between the measured and model-calculated amplitudes. R_{free} is the agreement for cross-validation data set. [d]The observation-to-parameter ratio (R_{o2p}) is defined by the number of unique observation by the number of refinement parameters, which is four times the number of atoms. [e]Root mean squares deviations (rmsd) to ideal values.

haven National Laboratory (BNL, Long Island, NY). The data were processed using the HKL2000 program suite,[26] as summarized in Table 1, Tables S1 and S2 (Supporting Information). Because we already had a very accurate structure of the RB69pol ternary complex at 1.8-Å resolution with free R-factor of 20.1% (pdb accession 3NCI)[23] as a starting model for this study and we did not expect any major structural changes, we used more conservative approaches in data processing with the $I/\sigma I > 1$ criteria for the highest resolution shell (Table S1,S2) than we have previously recommended (with the $F/\sigma F$ of about 1 as criteria).[27,28] All structures were solved by the automated molecular replacement method Phaser,[29] using 3NCI model after removing dCTP, DNA duplexes and all water molecules. The P/T DNA duplex and the incoming dNTP were built using the program COOT[30] into residual difference Fourier maps, which were phased with the partially refined polymerase model. The structure was refined using Refmac5,[31] as summarized in Table 1. Figures were made using the programs Ribbons and Pymol.[32,33]

PDB Accession Numbers. Coordinates and X-ray diffraction data for the all four complexes containing dF/dATP, dF/dGTP, dF/dCTP, and dF/dTTP are available from Protein Data Bank under accession numbers of 3QER, 3QES, 3QEI, and 3QEP, respectively. A part of the dF/dTTP-containing structure has already been described previously,[22] which entry is cited here for the complete set of all four-possible dNTP complexes.

Chemical Quench Experiments. Rapid chemical quench experiments were performed at 23 °C using the Kin-Tek rapid-quench flow instrument (model RQF-3) with a buffer solution of 66 mM Tris-HCl at pH 7.4 and 10 mM $MgSO_4$ and quenched with 0.5 M EDTA; K_d and k_{pol} values were determined using single-turnover conditions with the enzyme in 10-fold excess over the P/T, where [enzyme] was 1 μM and [P/T] was 83 nM. For each K_d and k_{pol} determination, seven different concentrations of the dNTP were used as described.[23,25] Data from single-turnover experiments fit well to the following equation with a single exponential term (Figures S1−S3): $[DNA] = A[1 - \exp(-k_{obs}t)]$, where k_{obs} is the observed rate constant, t is the elapsed constant, and A is a constant. The kinetic parameters, k_{pol} (the maximum rate of dNMP incorporation) and K_d^{app} (defined as the [dNTP] that provides an insertion rate that is 1/2 of the maximum rate that could be attained under conditions of saturating substrate), were obtained by fitting plots of k_{obs} versus [dNTP] to the equation $k_{obs} = k_{pol}[dNTP]/(K_d^{app} + [dNTP])$, as summarized in Tables 2−4.

RESULTS AND DISCUSSION

Kinetic Preference for Nucleotide Incorporation Opposite dF and Primer-Extension Beyond a dF/dN Pair at the P/T Junction. We had previously determined presteady-state kinetic parameters for incorporation of dAMP opposite dF by wt RB69pol in order to examine the contribution of interbase W−C HBs during DNA synthesis, under the assumption that dF was a nonpolar isostere of dT incapable of H-bonding.[19] These results now require reinterpretation based on our finding that dF is actually an

Table 2. Presteady-State Kinetic Parameters for Incorporation of dNMPs Opposite dF Catalyzed by wt and tm RB69pols[a]

dNTP/dF	pol	k_{pol} (s^{-1})	K_d^{app} (μM)	k_{pol}/K_d (μM^{-1} s^{-1})	(k_{pol}/K_d) ratio
dATP/dF	wt	1.8	2100	8.7×10^{-4}	1
dGTP/dF	wt	1.6×10^{-3}	2060	7.8×10^{-7}	1/1120[b]
dCTP/dF	wt	2.7×10^{-3}	>2500	6×10^{-7}	1/1450[b]
dTTP/dF	wt	1.2×10^{-1}	>2500	2.4×10^{-6}	1/360[b]
dATP/dT	wt	220	50	4.4	5057/1[c]
dATP/dF	tm	188	116	1.6	1
dGTP/dF	tm	16	1700	9×10^{-3}	1/180[b]
dCTP/dF	tm	36	>2500	1.3×10^{-2}	1/120[b]
dTTP/dF	tm	67	2400	2.8×10^{-2}	1/60[b]
dATP/dT	tm	300	60	5	3/1[c]

[a]The standard deviation was ±15% when the values were less than 100 μM, ± 25% when the values were between 100 and 1000 μM, and ±50% when the values were above 1 mM. The standard deviation for k_{pol} values were ±10%. [b]$(k_{pol}/K_d)_{dATP/dF}/(k_{pol}/K_d)_{dNTP/dF}$, (dNTP: dGTP, dCTP, or dTTP). [c]$(k_{pol}/K_d)_{dATP/dT}/(k_{pol}/K_d)_{dATP/dF}$.

isostere of dT but with H-bonding capability.[22] Since we have determined the structures of all four-possible dNTP/dF ternary complexes (Table 1), we decided to extend our presteady-state kinetic studies to include the incorporation of all four dNMPs opposite dF for both tm and wt RB69pols (Table 2, Figure S1–S4). Our data show that there exists a strong kinetic preference for incorporation of dAMP opposite dF versus the other three dNMPs for both wt and tm RB69pols (Table 2), but the preference for insertion of dAMP is almost 10-fold more pronounced with wt than with tm.

Having determined the effect of a templating dF on the kinetic behavior of both wt and the more permissive tm RB69pols, we were interested in defining the kinetic behavior of tm in primer-extensions when there was a dN/dF pair at the P/T junction (Table 3). We have shown that only the dA/dF pair allowed extension, albeit with drastically reduced efficiency compared to P/T junctions with correctly paired bases (Table 3). The efficiency for extension past the other three dN/dF pairs at the P/T junction was about 200 times lower than extension beyond the dA/dF pair. These differences are comparable to those found when mispairs occupy the terminal position of a P/T junction.[23]

Table 3. Presteady-State Kinetic Parameters for Primer-Extension beyond dNMP/dF with the Correct Incoming dCTP Opposite the Templating dG by tm RB69pol[a]

P/T junction	k_{pol} (s^{-1})	K_d (μM)	k_{pol}/K_d (μM^{-1} s^{-1})
dA/dF	6.21×10^{-2}	140	4.40×10^{-4}
dG/dF	5.02×10^{-3}	2730	1.83×10^{-6}
dC/dF	2.37×10^{-3}	1340	1.77×10^{-6}
dT/dF	5.78×10^{-3}	2050	2.82×10^{-6}

[a]The template base opposite to the priming nucleotide in P/T was replaced with dF in this assay. The standard deviation was ±15% when the values were less than 100 μM, ±25% when the values were between 100 and 1000 μM, and ±50% when the values were above 1 mM. The standard deviation for k_{pol} values were ±10%.

To identify which amino acid replacements in tm RB69pol are responsible for increased incorporation efficiency of dAMP opposite dF, we determined presteady-state kinetic parameters for each of the following RB69pol variants (Table 4): the S565G, L561A, and Y567A single mutants and the L561A/Y567A and S565G/Y567A double mutants. We found that the Y567A substitution has the dominant effect on the kinetic behavior in all combinations of single and double mutants as well as in tm. When the Y567A substitution is present, the incorporation efficiency of dAMP opposite to dF is greatly increased (Table 4, Figure S4). Similarly, this substitution also has a dominant effect on increased incorporation efficiency of incorrect dNMPs opposite a natural templating nucleotide, demonstrating the important role of the wt Y567 side chain in base selectivity.[20,23,25]

Table 4. Presteady-State Kinetic Parameters for Incorporation of dAMP opposite dF Catalyzed by wt RB69pol and Its NBP Mutants[a]

pol	k_{pol} (s^{-1})	K_d^{app} (μM)	k_{pol}/K_d (μM^{-1} s^{-1})
wt RB69pol	1.8	2100	8.7×10^{-4}
S565G	1.4	1900	7.4×10^{-4}
L561A	11	1800	6×10^{-3}
Y567A	133	596	0.2
Y567A/L561A	183	168	1.1
Y567A/S565G	123	1300	9.2×10^{-2}
Y567A/L561A/S565G	188	116	1.6

[a]The template base opposite the priming nucleotide in P/T was replaced with dF in this assay. The standard deviation was ±15% when the values were less than 100 μM, ±25% when the values were between 100 and 1000 μM, and ±50% when the values were above 1 mM. The standard deviation for k_{pol} values were ±10%.

Structural Overview of the dF/dNTP-Containing tm RB69pol Ternary Complexes. The structures of the four-possible dF/dNTP ternary complexes have been determined at sufficiently high resolutions (Table 1), including an earlier reported dF/dTTP ternary complex.[22] This has enabled us to correlate kinetic parameters with corresponding structural features in great detail. These structures reveal multiple layers of hydration surrounding the nascent base-pairs. At 1.8-Å resolution, as determined for the dF/dTTP-containing tm ternary complex[22] and the dG/dCTP-containing wt ternary complex,[23] we were able to observe at least three layers of hydration. For the three structures described here at resolutions near 2.0 Å (Table 1), distinct hydration networks have also been observed with all exposed polar groups involved in polar–polar interactions or via HBs (Figure 2). The exposed nonpolar groups were devoid of a first layer of hydration within their van der Waals contact radii. Beyond these radii, a rigid network of ordered water molecules was often observed to form a cage surrounding nonpolar groups such as the C5 methyl group of dT in DNA duplexes (Figure 2F) and nonpolar protein side chains at distances equivalent to the second hydration layer.[23]

The overall structures of all four ternary complexes containing dF are identical to the dG/dCTP-containing wt RB69pol ternary complex (Figure 1C). The root-mean-squares Cα deviation between the highest resolution ternary complex structures of the tm RB69pol (containing dF/dTTP) and the wt RB69pol (containing dG/dCTP) is 0.19 Å (excluding the last ten residues at the C-terminal tail), suggesting that three substitutions in the NBP of tm did not alter the enzyme structure. All four dF/dNTP-containing structures were completely superimposable, suggesting that the pol active site can accept all four dF/dNTP pairs without requiring any large structural rearrangements. The structures of the tm ternary complexes containing dF/dATP, dF/dGTP, or dF/dCTP were

dx.doi.org/10.1021/bi2016487 | Biochemistry 2012, 51, 1476–1485

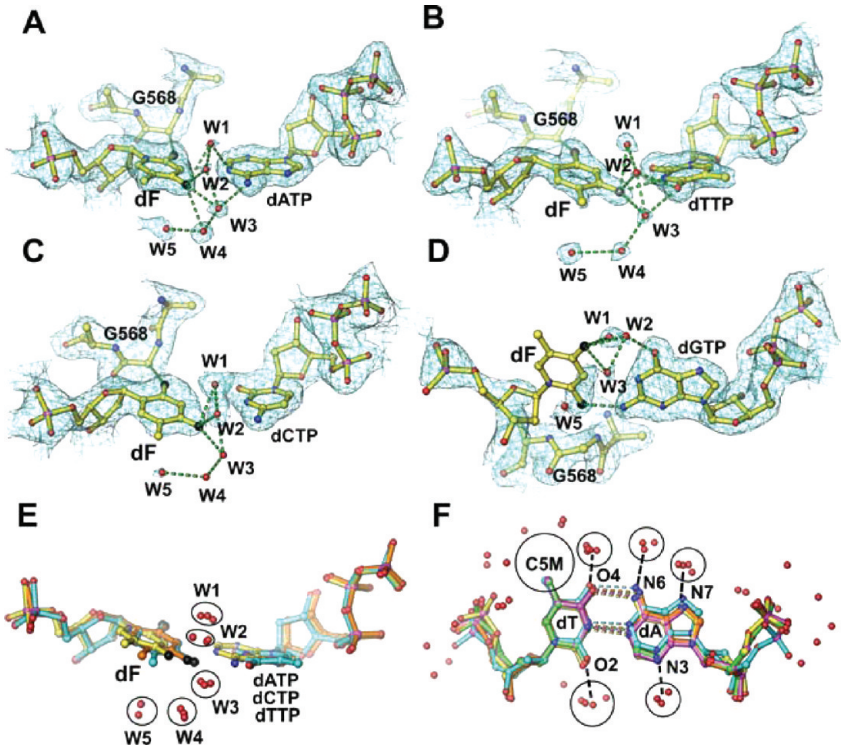

Figure 2. Structures of the dF/dNTP nascent base-pairs in the ternary complexes of tm RB69pol. (A) Final 2Fo-Fc electron density map at 1.96-Å resolution for the dF/dATP structure contoured at 1.2 σ (cyan chicken wires) superimposed on the refined model (yellow balls and sticks). HBs as defined by the donor−acceptor distance less than 3.2 Å are shown by dashed lines, and five ordered water molecules are named as W1 to W5. (B) Final 2Fo-Fc type map at 1.8-Å resolution for the dF/dTTP structure contoured at 1.0 σ.[22] (C) Final 2Fo-Fc type map at 2.18-Å resolution for the dF/dCTP structure contoured at 1.0 σ. (D) Final 2Fo-Fc map at 1.98-Å resolution for the dF/dGTP structure contoured at 1.0 σ. Densities for W4 exist at lower contoured levels (not shown). (E) Superposition of RB69pol Cα coordinates of the three complexes (dF/dATP, yellow; dF/dTTP, golden; and dF/dCTP, cyan) shows a conserved hydration network of five ordered water molecules (encircled). (F) Superposition of five dT/dA base pairs (at 2, 3, 4, 7, and 9 positions from the P/T junction, colored by yellow, golden, cyan, magenta, and green, respectively) in the P/T duplex of the dF/dTTP structure[22] reveals a conserved hydration network (encircled) surrounding the base pairs. The absence of water molecules next to C5M is indicated by a large circle.

determined at 1.96-Å, 1.98-Å, and 2.18-Å resolution, respectively, with free R-factors varying from 21.6 to 23.8% (Table 1). In all of these structures (Figure 2A-D), the electron densities for the templating dF residues and the surrounding network of ordered water molecules were well-defined except for the ternary complex with dGTP (Table S3). In that structure, the electron density for the templating dF with relatively high B-factors was less well-defined than it was for the incoming dGTP (Figure 2C, Figure S5). The average B factor for the dF's base analogue and dGTP's base is 52.1 and 20.8 Å^2, and the average B factor for the entire dF/dGTP complex is 28.5 Å^2. The average B factor for dF in this structure is still smaller than the overall B-factor (61.1 Å^2) for the entire ternary complex of the previously reported structure (1IG9) at 2.6-Å resolution.[34] In all these complexes (Figure 3), the triphosphate tail of dNTPs was in the catalytically relevant α,β,γ-tridendate coordination state.[24]

Novel Hydrogen Bonding Capability of the Templating dF. In the four dF-containing structures, both the F4 and F2 atoms of dF interact with polar groups (Figure 2). The exposed F4 group of the dF/dNTP base-pairs has several ordered water molecules (Table S3) located within 3.2 Å of its contact radii. These water molecules likely serve as HB donors. In addition, F4 accepts the N3−H of an incoming dTTP to form a direct HB (Figure 2B). Similarly, F2 accepts the N2−H of an incoming dGTP to form a direct HB (Figure 2D). F2 is also within 3.2 Å of the Cα-H of G568 in two of the dF-containing ternary complexes. In contrast, the C3−H of dF does not contact any polar groups and has no surrounding ordered water molecules (Figure 2F). By comparison, all known polar groups of natural nucleotides (for example, N1, N3, N6, and N7 of dA and O2 and N3 of dT) always interact with ordered water molecules or form interbase HBs (Figure 2F). Based on our structures, dF does not fit the criteria expected for a nonpolar, non-H bonding isostere of dT even though dF has a shape very similar to dT (Figure 1A,B). Because F2 and F4 of dF are within 3.2 Å, or less, of HB donors, it appears that these fluorine groups can act as HB acceptors, similar to O2 and O4 of dT (Figure 2). However, the C3−H moiety of dF does not form a HB in any of the four complexes, differing from the N3−H of dT (Figure 2). Thus, dF appears to be only a partially polar isostere of dT.

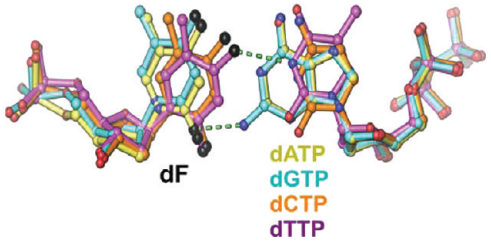

Figure 3. Overview of the four dF/dNTP complexes after superposition of the RB69pol Cα coordinates.

dx.doi.org/10.1021/bi2016487 | *Biochemistry* 2012, 51, 1476−1485

The fact that the F4/N6 pair of dF/dATP does not form an interbase HB in the environment of a pol active site suggests that the energetic contribution to the stability of the ternary complex from such an HB is relatively small. The formation of the F4/N6 interbase HB by itself was unable to compensate for the energetic cost of displacing all the ordered water molecules that surround F4 in the complex. An implication of this finding from substituting a modified base-pair for a natural base-pair is that the solvent-accessible O4/N6 interbase HB in the dT/dATP nascent base-pair is likely to contribute substantially less energy to the stabilization of the ternary complex than its buried N1/N3 interbase HB.

Differences between dF/dNs in DNA Duplexes and dF/dNTPs in the Pol Active Site. Within isolated DNA duplexes, the polarity of F2, C3, and F4 substituent of dF cannot be unambiguously discerned because some unfavorable polar/nonpolar interactions involving dF can be tolerated when there are strong physical constraints from phosphodiester linkages on both strands in DNA duplexes and from base-stacking on both sides of the nucleobases. The inability of dF to exhibit its polar potential in this situation may be why the shape of the dF/dA pair was observed to be similar to that of dT/dA.[7,9,15] The environment of the pol's NBP is very different from that found in an isolated DNA duplex. In the pol ternary complex, only one side of the nascent base pair is stacked against the penultimate base pair of the DNA duplex, while the other side includes unusual polar-nonpolar interactions between the side chain of S565 and the templating base in wt RB69pol.[23] Although the base of the incoming dNTP interacts with several hydrophobic side chains in wt RB69 pol, including L561, these interactions lack shape complementarity. In tm RB69pol, some of these interactions have been altered. Finally, the most important difference between modified nucleobases in an isolated DNA duplex and those in the pol active site is that the incoming dNTP is not constrained by a phosphodiester linkage.

We have shown above that the F4 substituent of dF has H-bonding capability in the RB69pol active site. However, it does not form an interbase HB with dATP, because the corresponding N6−H/F4 distance in the dF/dATP complex is 3.9 Å, which is outside the typical range of an interbase HB. Instead, it remains H-bonded to surrounding ordered water molecules (Figure 2A). A similar H-bonding pattern was observed recently in the dF/dATP-ternary complex of the RB69pol Y567A mutant (Figure S6).[22] The inability of the F4 substituent to displace surrounding ordered water molecules to form an interbase HB is due to an unfavorable nonpolar (C3−H) and polar (N1) interaction between dF and dATP, an interaction that was tolerated when dF/dA was embedded in an isolated DNA duplex (Figure 4A,B).

In addition, a strong F2/N2 nonwobble HB was also observed previously with a dF/dG base-pair in an isolated DNA duplex.[35] In that case, base stacking with flanking base-pairs prevented any twisting of dF as seen here in the RB69pol active site. This extra stacking interaction compensates for the repulsive C3H−N1H interaction where two H atoms point 45° away from each other, avoiding a steric clash, although the interatomic C3/N1 distance (3.25 Å) remains relatively short (Figure 4C,D).

Shape Differences between dF/dNTPs and Corresponding dT/dNTPs. We have also determined the structures of tm ternary complexes containing each of the four-possible dNTPs opposite dT at resolutions varying from 1.73 to 2.08 Å.

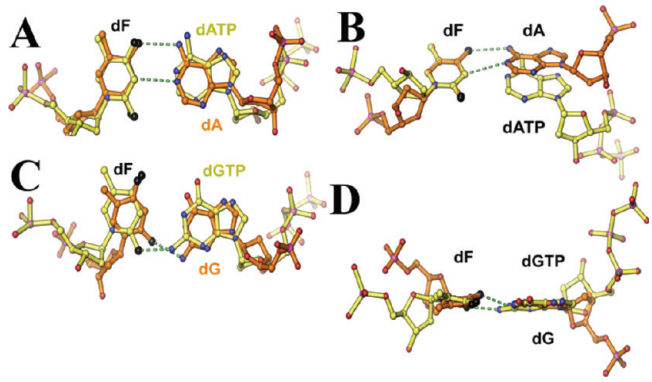

Figure 4. Shape differences between dF/dNTPs within the tm ternary complexes and the corresponding of dF/dN embedded in the middle of isolated DNA duplexes.[15,34] (A-B) Two orthogonal views of dF/dATP (yellow) versus dF/dA (golden). (C-D) Two orthogonal views of dF/dGTP (yellow) versus dF/dG (golden).

Analysis of these structures is beyond the scope of this report. Nevertheless, they provide a basis for shape comparisons between dF/dNTPs and the corresponding dT/dNTPs when they are situated in the NBP of RB69pol. By comparison, it becomes clear that the shapes of the nascent dF/dNTPs are very different from their nascent dT/dNTP counterparts (Figure 5). This is consistent with our observation that dF does not behave as a hydrophobic isostere of dT. In the dF/dATP ternary complex (Figure 5A), there are no direct interbase HBs between dF and dATP in the RB69pol active site, which stands in sharp contrast to the shapes of dF/dA and dT/dA pairs when they are embedded in an isolated DNA duplex.[7,9,15]

In the dF/dGTP complex, an interbase F2/N2−H non-wobble HB is observed with an interatomic distance of 2.55 Å, whereas the corresponding nascent dT/dGTP and dG/dTTP mispairs have two wobble HBs (Figure 5B). The F2/N2−H HB reduces the C3−N1 distance to 3.3 Å between dF's C3 and dG's N1 where their H atoms would sterically clash (Figure 5B). This is consistent with the observation of only partially ordered dF in the dF/dGTP complex because of a single F2/N2 HB with no additional HB anchoring point between F2 of dF and the Cα-H of G568 (3.6 Å), an interaction which is present in many other RB69pol ternary complexes.[23−25]

With respect to the two remaining dF-containing ternary complexes that have pyrimidine bases opposite dF, we have shown that the shapes of dF/dTTP and dF/dCTP pairs resemble one another (Figure 3, 5C,E). C3−H of dF in both structures was able to avoid contact with any polar groups because dF was tilted toward dTTP or dCTP so that ordered water molecules could not be inserted at the interface between the bases (Figure 5C,E). Thus, C3−H of dF in these complexes remains buried. There is no interbase HB in the dF/dCTP complex, but a wobble HB was observed between F4 and N3−H in the dF/dTTP complex. In contrast, the dT/dCTP complex has three ordered water molecules at the interface that mediates their interbase HBs, and the dT/dTTP pair has two wobble interbase HBs (Figure 5D,F).

Structural Basis for dF's Kinetic Preference. Our kinetic data have shown that the catalytic efficiency for incorporation of dAMP opposite dF by tm RB69pol is 180, 120, and 60 fold greater than that of dGMP, dCMP, and dTMP, respectively (Table 2). The kinetic preference for incorporation of dAMP opposite dF is consistent with the corresponding structures

dx.doi.org/10.1021/bi2016487 | *Biochemistry* 2012, 51, 1476−1485

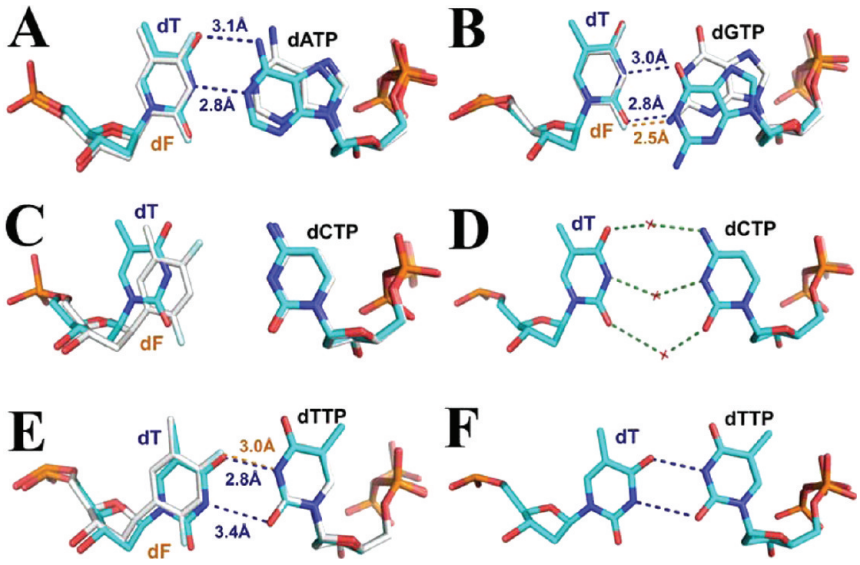

Figure 5. Shape differences between dF/dNTPs and the corresponding dT/dNTPs within the ternary complexes of tm RB69pol. (A) dF/dATP (gray) versus dT/dATP (blue). (B) dF/dGTP (gray) versus dT/dGTP (blue). (C) dF/dCTP (gray) versus dT/dCTP (blue). (D) dT/dCTP. (E) dF/dTTP (gray) versus dT/dTTP (blue). (F) dT/dTTP. All superposition was made for comparison using polymerase Cα coordinates. All putative interbase HBs are indicated by distances (blue for dT/dNTPs and orange for dF/dNTPs).

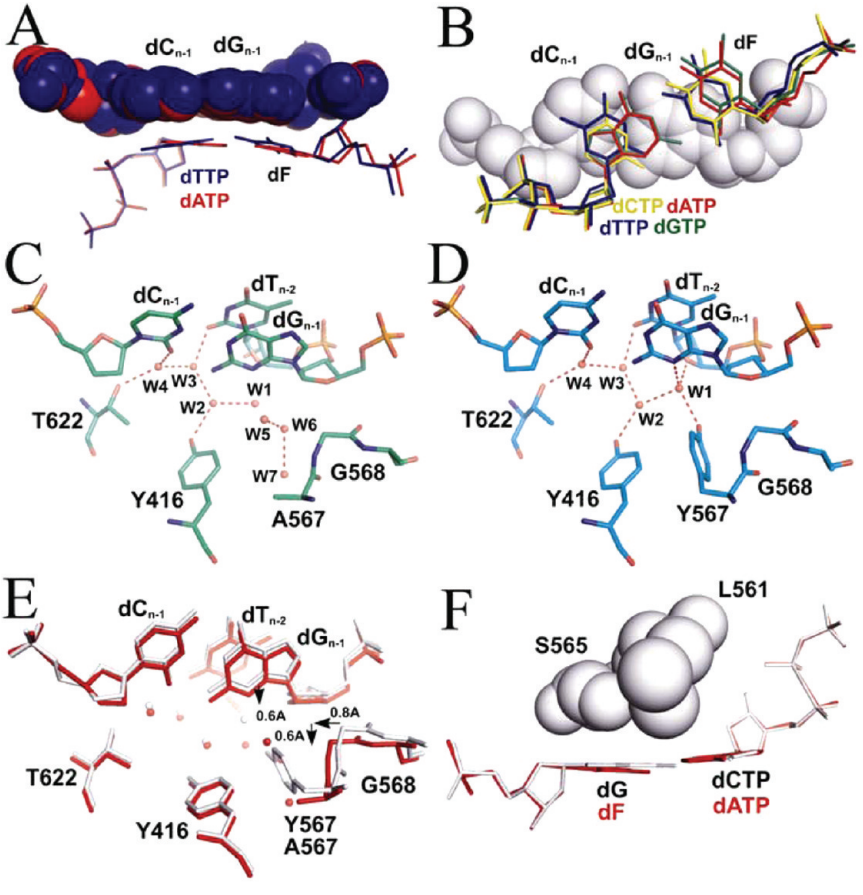

Figure 6. Structural basis for preferential kinetic incorporation of dNMPs opposite dF. (A) Superposition of the RB69pol Cα coordinates of the dF/dATP (red) and dF/dTTP (blue) complexes. The penultimate base-pair is shown in space-filling mode. (B) Superposition of the RB69pol Cα coordinates of all four complexes, dF/dATP (red), dF/dTTP (blue), dF/dCTP (yellow), and dF/dGTP (green). (C) Overview of the NBP of tm RB69pol in the dF/dATP complex. A more flexible nucleotide binding pocket is produced by three amino acid substitutions in tm RB69pol than in wt RB69pol. Please note that ordered water molecules labeled as W1 through W7 in this figure differ from those in Figure 2. (D) The NBP of the dG/dCTP-containing wt RB69pol complex with rigid HB network at the minor groove of the primer/template DNA duplex.[23] (E-F) Two orthogonal views of superposition of C and D: dF/dATP (gray) and dG/dCTP (red) in stick and surface representations.

dx.doi.org/10.1021/bi2016487 | *Biochemistry* 2012, 51, 1476–1485

described here (Figure 6). In brief, we show that the shape of dF/dGTP is similar to that of dF/dATP (Figure 3). Both nascent base-pairs involving purine dNTPs exhibit more extensive stacking with the penultimate base pair when they are compared to the dF/dCTP or dF/dTTP pyrimidine pairs (Figure 6A,B). Because C3−H of dF has no HB donor capability, dF/dGTP cannot form dT/dGTP-like wobble HBs. Instead, it forms a nonwobble F2/N2−H HB. To avoid the repulsive interaction between dF's C3−H and dGTP's N1−H, dF undergoes a large twisting motion as evident from its poor electron density and relatively large B-factors (Figure 2C). This twisting motion could destabilize the ternary complex and introduce further distortion in substrate alignment. It could also explain why dGMP, when opposite dF, has the lowest incorporation efficiency in the tm RB69pol catalyzed reaction (Table 2).

In both the dF/dCTP and dF/dTTP complexes, the templating dF has been reoriented burying its hydrophobic C3−H to avoid any direct contact with polar groups such as ordered water molecules (Figure 6D). The C3−H of dF points between O2 and N1 of dCTP or next to O2 of dTTP. This reorientation results in greater destabilization of this ternary complex than with dF/dATP where no major reorientation of dF occurs relative to the situation obtained with the corresponding dT/dATP complex. Although F2 of dF forms the same HB with Cα-H of G568 in both the dF/dCTP and dF/dTTP complexes, the F4 substituent of dF in the dF/dTTP complex forms an interbase HB with N3−H of dTTP but cannot do so with N3 of dCTP in the dF/dCTP complex. This extra HB could account for the 2 fold increase in catalytic efficiency for incorporation of dTMP versus dCMP opposite dF (Table 2).

A paradox remains in that the insertion of dAMP catalyzed by tm RB69pol is 3 times more efficient than the insertion of dTMP opposite dF (Table 2), even though dATP/dF has one less HB than dTTP/dF. The kinetic behavior is not solely determined by the number of interbase HBs, but by other factors as well such as base-pair stacking. Indeed, there is a better stacking with the penultimate base pair in the dF/dATP complex than in the dF/dTTP complex (or in the dF/dCTP complex) (Figure 6A). Clearly with dF/dATP, base-pair stacking makes a greater contribution to the kinetics than interbase HBs. However, base-pair stacking between dF/dATP and the penultimate base pair is not optimal when compared to the dT/dATP base pair (Figure 6A). Due to the absence of the C3−H/N1 and F4/N4 HBs, the dF/dATP pair also has a relatively large buckle relative to dT/dATP (Figure 6A), which reduces the extent of base pair stacking. This buckling likely diminishes the stability of the ternary complex and would be expected to reduce the incorporation efficiency of dAMP opposite dF relative to dAMP opposite dT (Table 2). This buckling does not occur when dF/dA is embedded in an isolated DNA duplex.[7,9,15]

Our previous structural studies have shown that there is a rigid HB network at the minor groove of the nascent P/T duplex.[23] This network includes five ordered water molecules, four of which are immediately adjacent to the penultimate base pair (labeled W1 to W4 in Figure 6D). It also includes the side chain hydroxyl groups of Y567, Y416, and T622 (Figure 6D). By replacing Y567 with Ala, this rigid HB network was disrupted, and the space generated by removing the hydroxyphenyl group of Y567 is now occupied by three additional water molecules (labeled W5 to W7 in Figure 6C).[23] In addition, the water molecule W1 is no longer within HB distance of N3 in dG of the penultimate base pair in the template strand. Least squares superposition of the wt and tm structures shows that: (i) the dG base at the N-1 position of the template strand recedes into the DNA minor groove by 0.6 Å relative to wt largely due to the removal of the Y567 side chain and to the corresponding altered hydration network in tm (Figure 6); (ii) the A567 and G568 main chains shift 0.8 Å laterally toward the Y416 side chain, and 0.6 Å vertically toward the minor groove relative to wt (Figure 6E) and; (iii) the minor groove of the nascent base pair in the tm complex contacts two (or three[23]) ordered water molecules, whereas it is sequestered from any water molecules in the wt complex. The dehydration of the nascent base pair could explain the 2,000-fold increase of dAMP incorporation opposite dF by tm than by wt (Table 2). In addition, in the wt structure,[23] the side chains of S565 and L561 interact with the aromatic plane of the templating base. The enlarged NBP in tm permits the nascent base-pair to have a larger buckling angle than would be possible with wt RB69pol (Figure 6F). Overall, the disruption of HB networks by the Y567A substitution (Figure 6, Figure S6) provides more flexibility in the NBP and is consistent with increased incorporation efficiency for all of the dNMPs opposite dF by 10^3 to 10^4 fold exhibited by tm relative to the wt enzyme. This structural feature is consistent with the observation that the Y567A substitution has a dominant effect on misincorporation kinetics in all combinations of NBP mutants that contain this replacement (Table 4, Figure S1−S4).

We predict that chemical and structural properties of dF/dN pairs in the penultimate base-pair position of the P/T duplex will differ from dF/dNTP pairs in the NBP of all pol active sites as well as from the dF/dN pairs embedded in isolated DNA duplexes. After translocation of the P/T duplex following dF incorporation, dF/dA now moves to the penultimate base pair position and would have more extensive base-pair stacking within the P/T duplex than dF/dC and dF/dT or dF/dG. The dF/dG pair has a strong repulsive C3/N1 interaction that prevents effective base-pair stacking. All these predictions are consistent with our primer-extension kinetics with dF/dN at the terminus of the P/T duplex (Table 4). In fact, Irimia et al.[16] confirmed our predictions when they determined corresponding structures of Dpo4 ternary complexes showing that the shapes of dF/dN embedded in isolated DNA duplexes indeed differ from those at the end of a DNA duplex or at the penultimate base-pairing position of the P/T duplex complexed with Dpo4 (Figure 7). Of course the geometry of base-pairs involving dF in the environment of the Dpo4 active site is also likely to be different from that of RB69pol.

Taken together, the structures of the four-possible dF/dNTP complexes in a complete set, described here, provide evidence that a templating dF can form novel HBs that differ from those involving a templating dT. This was not anticipated since the chemical properties of dF, determined in DNA duplexes in the absence of a polymerase, indicated that it was nonpolar and unable to participate in HB interactions.[5−12,21] Although dF is an isostere of dT, its H-bonding capability is likely to be responsible for the unusual shapes and geometry of nascent dNTP/dF pairs that are not isosteric with their corresponding nascent dNTP/dT pairs.

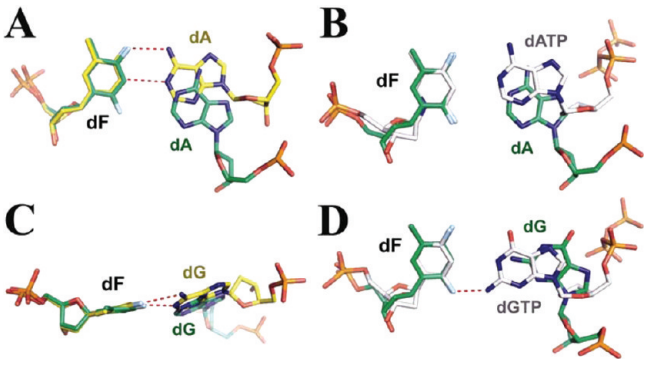

Figure 7. Shape differences between dF/dNs at the penultimate base pairing position of the P/T duplex of dpo4[16] and the corresponding dF/dN embedded inside isolated DNA duplexes[15,34] or between the dpo4 and tm RB69pol ternary complexes. (A) dF/dA at the penultimate base pairing position (green) versus dF/dA embedded in DNA (yellow). (B) dF/dA at the penultimate base pairing position (green) versus dF/dATP (gray). (C) dF/dG at the penultimate base pair position (green) with dF/dG embedded in DNA (yellow). (D) dF/dG at the penultimate base pairing position (green) versus dF/dGTP (gray).

■ ASSOCIATED CONTENT

Supporting Information

Additional three tables and six figures. This material is available free of charge via the Internet at http://pubs.acs.org.

■ AUTHOR INFORMATION

Corresponding Author

*Phone: (203)-432-5737. E-mail: jimin.wang@yale.edu (J.W.). Phone: (203)-785-5499. E-mail: william.konigsberg@yale.edu (W.K.).

Funding

This work was supported by NIH RO1-GM063276-09 (to W.H.K.), by SCSB-GIST (to S.H.E and J.W.), and by NRF-20110016226 (to S.H.E.)

Notes

The authors declare no competing financial interest.

■ ACKNOWLEDGMENTS

We thank the staff of the NE-CAT beamline 24-ID-E at the Advanced Photon Source of Argonne National Laboratory and of X29 of National Synchrotron Light Source at the Brookhaven National Laboratory.

■ ABBREVIATIONS

pol, DNA polymerase; RB69pol, bacteriophage RB69 DNA polymerase; dF, 2,4-difluorotoluene nucleoside analogue; NBP, Nascent basepair-Binding Pocket; W−C base-pair, Watson−Crick base-pair; P/T, primer/template DNA duplex; H bond or HB, hydrogen bond; wt, wild type; tm, triple mutant harboring L561A/S565G/Y567A substitutions; dNTPs, 2′-deoxynucleoside 5′-triphosphates; dNMPs, 2′-deoxynucleoside 5′-monophosphate; PEG 350 MME, polyethylene glycol 350 monomethyl ether

■ REFERENCES

(1) Echols, H., and Goodman, M. F. (1991) Fidelity mechanisms in DNA replication. *Annu. Rev. Biochem. 60*, 477−511.

(2) Kunkel, T. A. (1992) DNA replication fidelity. *J. Biol. Chem. 267*, 18251−18254.

(3) Goodman, M. F., Creighton, S., Bloom, L. B., and Petruska, J. (1993) Biochemical basis of DNA replication fidelity. *Crit. Rev. Biochem. Mol. Biol. 28*, 83−126.

(4) Kunkel, T. A., and Bebenek, K. (2000) DNA replication fidelity. *Annu. Rev. Biochem. 69*, 497−529.

(5) Moran, S., Ren, R. X., and Kool, E. T. (1997) A thymidine triphosphate shape analog lacking Watson-Crick pairing ability is replicated with high sequence selectivity. *Proc. Natl. Acad. Sci. U. S. A. 94*, 10506−10511.

(6) Guckian, K. M., and Kool, E. T. (1997) Highly precise shape mimicry by a difluorotoluene deoxynucleoside, a replication-competent substitute for thymidine. *Angew. Chem., Int. Ed. Engl. 36*, 2825−2828.

(7) Guckian, K. M., Krugh, T. R., and Kool, E. T. (1998) Solution structure of a DNA duplex containing a replicable difluorotoluene-adenine pair. *Nat. Struct. Biol. 5*, 954−959.

(8) Morales, J. C., and Kool, E. T. (1998) Efficient replication between non-hydrogen-bonded nucleoside shape analogs. *Nat. Struct. Biol. 5*, 950−954.

(9) Guckian, K. M., Schweitzer, B. A., Ren, R. X., Sheils, C. J., Tahmassebi, D. C., and Kool, E. T. (2000) Factors contributing to aromatic stacking in water: evaluation in the context of DNA. *J. Am. Chem. Soc. 122*, 2213−2222.

(10) Kool, E. T., and Sintim, H. O. (2006) The difluorotoluene debate--a decade later. *Chem. Commun. (Cambridge, U. K.)*, 3665−3675.

(11) Liu, D., Moran, S., and Kool, E. T. (1997) Bi-stranded, multisite replication of a base pair between difluorotoluene and adenine: confirmation by 'inverse' sequencing. *Chem. Biol. 4*, 919−926.

(12) Moran, S., Ren, R. X., Rumney, S., and Kool, E. T. (1997) Difluorotoluene, a nonpolar isostere for thymine, codes specifically and efficiently for adenine in DNA replication. *J. Am. Chem. Soc. 119*, 2056−2057.

(13) Lee, H. R., Helquist, S. A., Kool, E. T., and Johnson, K. A. (2008) Base pair hydrogen bonds are essential for proofreading selectivity by the human mitochondrial DNA polymerase. *J. Biol. Chem. 283*, 14411−14416.

(14) Schweitzer, B. A., and Kool, E. T. (1995) Hydrophobic, non-hydrogen-bonding bases and base pairs in DNA. *J. Am. Chem. Soc. 117*, 1863−1872.

(15) Pallan, P. S., and Egli, M. (2009) Pairing geometry of the hydrophobic thymine analogue 2,4-difluorotoluene in duplex DNA as analyzed by X-ray crystallography. *J. Am. Chem. Soc. 131*, 12548−12549.

(16) Irimia, A., Eoff, R. L., Pallan, P. S., Guengerich, F. P., and Egli, M. (2007) Structure and activity of Y-class DNA polymerase DPO4 from *Sulfolobus solfataricus* with templates containing the hydrophobic thymine analog 2,4-difluorotoluene. *J. Biol. Chem. 282*, 36421−36433.

(17) Lee, H. R., Helquist, S. A., Kool, E. T., and Johnson, K. A. (2008) Importance of hydrogen bonding for efficiency and specificity of the human mitochondrial DNA polymerase. *J. Biol. Chem. 283*, 14402−14410.

(18) Potapova, O., Chan, C., Delucia, A. M., Helquist, S. A., Kool, E. T., Grindley, D. F., and Joyce, C. M. (2006) DNA polymerase catalysis in the absence of Watson-Crick hydrogen bonds: analysis by single-turnover kinetcs. *Biochemistry 45*, 890−898.

(19) Braithwaite, D. K., and Ito, J. (1993) Compilation, alignment, and phylogenetic relationships of DNA polymerases. *Nucleic Acids Res. 21*, 787−802.

(20) Zhang, H., Beckman, J., Wang, J., and Konigsberg, W. (2009) RB69 DNA polymerase mutants with expanded nascent base-pair-binding pockets are highly efficient but have reduced base selectivity. *Biochemistry 48*, 6940−6950.

(21) Kool, E. T. (2002) Active site tightness and substrate fit in DNA replication. *Annu. Rev. Biochem. 71*, 191−219.

(22) Xia, S., Konigsberg, W. H., and Wang, J. (2011) Hydrogen-bonding capability of a templating difluorotoluene nucleotide residue in an RB69 DNA polymerase ternary complex. *J. Am. Chem. Soc. 133*, 10003−10005.

(23) Wang, M., Xia, S., Blaha, G., Steitz, T. A., Konigsberg, W. H., and Wang, J. (2010) Insight into base selectivity from the 1.8 Å resolution structure of an RB69 DNA polymerase ternary complex. *Biochemistry 50*, 581−590.
(24) Xia, S., Wang, M., Blaha, G., Konigsberg, W. H., and Wang, J. (2011) Structural insights into complete metal ion coordination from ternary complexes of B family RB69 DNA polymerase. *Biochemistry 50*, 9114−9124.
(25) Xia, S., Wang, M., Lee, H. R., Sinha, A., Blaha, G., Christian, T., Wang, J., and Konigsberg, W. (2011) Variation in mutation rates caused by RB69pol fidelity mutants can be rationalized on the basis of their kinetic behavior and crystal structures. *J. Mol. Biol. 406*, 558−570.
(26) Otwinowski, Z., and Minor, W. (1997) Processing of X-ray diffraction data collected in oscillation mode. *Methods Enzymol.*, 307−326.
(27) Wang, J., and Boisvert, D. C. (2003) Structural basis for GroEL-assisted protein folding from the crystal structure of (GroEL-KMgATP)14 at 2.0 Å resolution. *J. Mol. Biol. 327*, 843−855.
(28) Wang, J. (2010) Inclusion of weak high-resolution X-ray data for improvement of a group II intron structure. *Acta Crystallogr. D66*, 998−1000.
(29) McCoy, A. J., Grosse-Kunstleve, R. W., Adams, P. D., Winn, M. D., Storoni, L. C., and Read, R. J. (2007) Phaser crystallographic software. *J. Appl. Crystallogr. 40*, 658−674.
(30) Emsley, P., and Cowtan, K. (2004) Coot: model-building tools for molecular graphics. *Acta Crystallogr. D60*, 2126−2132.
(31) Murshudov, G. N., Vagin, A. A., and Dodson, E. J. (1997) Refinement of macromolecular structures by the maximum-likelihood method. *Acta Crystallogr. D53*, 240−255.
(32) Carson, M. (1991) Ribbons 2.0. *J. Appl. Crystallogr. 24*, 958−961.
(33) The PyMOL Molecular Graphics System, Version 1.2r3pre, Schrödinger, LLC.
(34) Franklin, M. C., Wang, J., and Steitz, T. A. (2001) Structure of the replicating complex of a pol α family polymerase. *Cell 105*, 657−667.
(35) Pfaff, D. A., Clarke, K. M., Parr, T. A., Cole, J. M., Geierstanger, B. H., Tahmassebi, D. C., and Dwyer, T. J. (2008) Solution structure of a DNA duplex containing a guanine-difluorotoluene pair: a wobble pair without hydrogen bonding? *J. Am. Chem. Soc. 130*, 4869−4878.